Pediatric Radiology (2022) 52:1326–1337
https://doi.org/10.1007/s00247-022-05298-7

ORIGINAL ARTICLE

Free-breathing magnetic resonance imaging with radial k-space sampling for neonates and infants to reduce anesthesia

Lorna P. Browne[1] · LaDonna J. Malone[1] · Erin K. Englund[1] · Takashi Fujiwara[1] · Chris Fluta[1] · Quin Lu[2] · Theresa R. Grover[3] · Peter G. Fuhr[4] · Alex J. Barker[1,5]

Received: 1 September 2021 / Revised: 17 December 2021 / Accepted: 20 January 2022 / Published online: 16 February 2022

Abstract

Background Conventional chest and abdominal MRI require breath-holds to reduce motion artifacts. Neonates and infants require general anesthesia with intubation to enable breath-held acquisitions.

Objective We aimed to validate a free-breathing approach to reduce general anesthesia using a motion-insensitive radial acquisition with respiratory gating.

Materials and methods We retrospectively enrolled children <3 years old who were referred for MRI of the chest or abdomen. They were divided into two groups according to MRI protocol: (1) breath-held scans under general anesthesia with T2-weighted single-shot fast spin-echo (SSFSE) and contrast-enhanced T1-weighted modified Dixon, and (2) free-breathing scans using radial sequences (T2-W MultiVane XD and contrast-enhanced T1-W three-dimensional [3-D] Vane XD). Two readers graded image quality and motion artifacts.

Results We included 23 studies in the free-breathing cohort and 22 in the breath-hold cohort. The overall imaging scores for the free-breathing radial T2-W sequence were similar to the scores for the breath-held T2-W SSFSE sequence (chest, 3.6 vs. 3.2, P=0.07; abdomen, 3.9 vs. 3.7, P=0.66). The free-breathing 3-D radial T1-W sequence also had image quality scores that were similar to the breath-held T1-W sequence (chest, 4.0 vs. 3.0, P=0.06; abdomen, 3.7 vs. 3.9, P=0.15). Increased motion was seen in the abdomen on the radial T2-W sequence (P<0.001), but increased motion was not different in the chest (P=0.73) or in contrast-enhanced T1-W sequences (chest, P=0.39; abdomen, P=0.15). The mean total sequence time was longer in free-breathing compared to breath-held exams (P<0.01); however, this did not translate to longer overall exam times (P=0.94).

Conclusion Motion-insensitive radial sequences used for infants and neonates were of similar image quality to breath-held sequences and had decreased sedation and intubation

Keywords Abdomen · Anesthesia · Breath-holding · Chest · Children · Infants · Magnetic resonance imaging · Radial · Sedation

✉ Lorna P. Browne
lorna.browne@childrenscolorado.org

[1] Department of Radiology, Section of Pediatric Radiology, Children's Hospital Colorado, University of Colorado Anschutz Medical Campus, 13123 East 16th Ave., Aurora, CO 80045, USA

[2] Philips Medical Systems, Best, the Netherlands

[3] Department of Pediatrics, Section of Neonatology, Children's Hospital Colorado, Aurora, CO, USA

[4] Division of Pediatric Anesthesiology, University of Colorado Anschutz Campus, 13123 East 16th Ave., Aurora, CO 80045, USA

[5] Department of Bioengineering, University of Colorado Anschutz Medical Campus, Aurora, CO, USA

Introduction

Pediatric chest and abdominal imaging have traditionally required breath-holding to mitigate image degradation that can result from respiratory motion. Because volitional breath-holding is not usually possible in young children, anesthesia is often necessary [1, 2]. Many children need multiple MRIs, each involving additional exposure to general anesthesia. With the increased awareness of potential neurocognitive effects of anesthesia on the developing brain of infants and children, significant efforts are ongoing to reduce the need for anesthesia in this vulnerable population [2–12]. The obstacles to adaptation of free-breathing techniques in this population include

high respiratory rates and a smaller field of view, which can result in undesirable signal-to-noise ratio. Recent advances in MRI technology, including multi-channel pediatric coils, faster three-dimensional (3-D) volumetric acquisitions with parallel imaging and compressed sensing, and more robust methods of respiratory compensation, have enabled the possibility to eliminate breath-holding and consequently reduce the duration, degree and overall use of anesthesia [13–15].

Most of the current focus on pediatric MR imaging is directed at accelerating imaging times by using techniques such as variable refocusing flip angles, partial Fourier techniques or novel k-space encoding trajectories [16–18]. The use of motion-insensitive radial acquisitions might reduce image artifacts, need for breath-holding and hence anesthesia in this patient population. For example, techniques such as periodically rotated overlapping parallel lines with enhanced reconstruction (PROPELLER, or MultiVane XD; Philips Healthcare, Best, the Netherlands) uses a modified radial k-space encoding pattern to mitigate motion artifacts [19]. MultiVane XD is commercially available and thus easily implemented in the clinical setting but is only applicable to two-dimensional (2-D) acquisitions. In addition, 3-D radial k-space trajectories, such as 3-D Vane XD on the Philips platform, are often used to encode k-space using radial spokes in a stack-of-stars sampling scheme, enabling 3-D approaches that are robust to motion [20].

In attempts to introduce free-breathing algorithms, we have experimented with free-breathing modifications to Cartesian sequences, but these modifications were at the sacrifice of image quality to a degree that prohibited widespread implementation. Prior studies have shown improved image quality and robustness to motion with radial approaches in adults [21–28]. Given promising adult studies and in the pursuit of high-quality free-breathing pediatric acquisitions, in 2019 our institution began investigating the use of free-breathing radial MRI sequences to reduce the number of children undergoing general anesthesia. As a result, our conventional breath-hold T1-weighted modified Dixon (mDixon) and T2-W single-shot fast spin-echo (SSFSE) acquisitions were replaced with a respiratory-navigated stack-of-stars mDixon approach (3-D Vane XD) and respiratory navigated T2-W PROPELLER (MultiVane XD) sequences. Our hypothesis was that the introducing these free-breathing radial sequences in our youngest MRI body patients could facilitate a reduction in the need for general anesthesia while maintaining diagnostic imaging quality.

Materials and methods

Study cohort and imaging

Our institutional review board approved this study under an existing approval for imaging studies related to quality improvement by the Colorado Multiple Institutional Review Board (COMIRB). We had a waiver of consent for this retrospective study.

We selected neonates and infants from consecutive clinically indicated MRI exams between 2017 and 2020, a time period that included 18 months before and after the introduction of the free-breathing radial sequences. Exams were performed on 1.5-tesla (T) or 3-T Ingenia or Elition X systems (Philips Healthcare). Inclusion criteria were children ages 3 years or younger undergoing MRI chest/abdomen examinations with axial fat-saturated T2-W and axial post-contrast (approximately 60 s after gadolinium administration) T1-W imaging. Additional sequences or planes performed as part of the child's indication-driven MRI protocol were not evaluated in this study. Children who only had non-contrast exams were excluded. We divided children into two comparison cohorts:

Cohort 1 (breath-hold Cartesian sequences) included children and infants (36 months and younger) who underwent an MRI of the chest or abdomen and had T2-W and contrast-enhanced T1-W imaging with SSFSE and mDixon techniques and sequential breath-holding (n=22). There were 9 chest examinations and 13 abdomen examinations in this cohort.

Cohort 2 (free-breathing radial sequences) included age-matched children and infants who underwent MRI of the chest or abdomen with both MultiVane XD (radial T2-W) and contrast-enhanced 3-D Vane XD (3-D radial with 160% radial coverage/116 phase encoding steps) sequences performed using respiratory navigation (n=23). There were 11 chest examinations and 12 abdomen examinations in this cohort.

Scan parameters are shown in Table 1 and patient demographics in Table 2.

Image interpretation and scan time computation

Qualitative imaging scoring of all children was performed by two pediatric radiologists (L.P.B., with 15 years of experience, and L.J.M., with 6 years of experience). MRI examinations were deidentified and reviewed independently in randomized order. The radiologists were blinded to the underlying diagnosis, imaging report and previous MRI examinations, as well as breath-held vs. free-breathing technique. They evaluated images for visualization of predefined anatomical features and the presence of artifacts. Qualitative image scores were based upon the clarity of the features of five thoracic anatomical landmarks (pulmonary arteries, trachea and mainstem bronchi, lung parenchyma, thymus and spinal cord) and five abdominal anatomical landmarks (portal veins, diaphragmatic crura, pancreas,

Table 1 Magnetic resonance imaging (MRI) sequence parameters

MRI parameters	T2-weighted sequences		Contrast-enhanced T1-W sequences	
	Single-shot fast spin echo	Radial (MultiVane XD)	Modified Dixon	3-D radial (3-D Vane XD)
Voxel size (mm)	1.4×1.4×3	1.3×1.3×3	1.2×1.2×2	1.2×1.2×1.3
Field of view (cm)	20	20	20	20
TR/TE (ms)	1,000/70	1,860/80	3.7/1.9	5.7/1.9
Flip angle (°)	90	90	10	10
Number of averages	1	1–2	1	1
Parallel imaging (freq/phase)	1.7/1	2/1	None	1/1
Respiratory motion compensation technique	Breath-hold	Respiratory navigator	Breath-hold	Respiratory navigator
Median scan time (s)	37	168	9	113

freq frequency, *TE* echo time, *TR* repetition time

Table 2 Patient demographics, examination and anesthesia status

	Breath-hold (n=22)	Free-breathing (n=23)	P-value[a]
Age			0.06
Age (y)	1.8±1.2	1.1±1.0	
Range (y)	[0.1–3.0]	[0.01–3.0]	
Gender, female	7 (31.8%)	15 (65.2%)	0.06
Indication			0.34
Tumor	10 (46.5%)	11 (47.8%)	
Vascular malformation	7 (31.8%)	7 (30%)	
Button battery ingestion	5 (22.7%)	2 (9%)	
Other		3 (13%)	
Field strength, 3 T	14 (63.6%)	20 (87%)	0.07
Body part			0.87
MRI chest exam	9 (40.9%)	11 (47.8%)	
MRI abdomen exam	13 (59.1%)	12 (52.2%)	
Patient status, inpatient	5 (22.7%)	8 (34.8%)	0.57
Anesthesia			**0.001**
General anesthesia with ETT	22 (100.0%)	3 (13.0%)	
Sedation with nasal cannula	0 (0.0%)	12 (52.2%)	
Sedation LMA	0 (0.0%)	3 (13.0%)	
Feed and swaddle	0 (0.0%)	5 (21.7%)	

ETT endotracheal tube, *LMA* laryngeal mask airway, *y* years

[a] $P<0.05$ is significant (bold)

adrenal gland and spinal cord) using a 5-point Likert scale (1 = not distinguishable, 2 = limited visibility, 3 = diagnostic visualization, 4 = good feature clarity, 5 = excellent feature clarity). The readers evaluated all images for the presence of motion artifacts based on a different 5-point Likert scale (1 = motion limiting assessment of most structures, 2 = motion limiting assessment of 3 or more structures, 3 = artifacts limiting assessment of 1–2 structures, 4 = minimal detectable artifacts, 5 = no detectable artifact). We determined an overall imaging score (1–5) based upon the means of anatomical and motion scores.

We calculated scan and sequence times from the Digital Imaging and Communications in Medicine (DICOM) header data and compared the mean and ranges across both cohorts in the following manner:

(1) *Total exam time* was calculated as the entire duration of the MRI examination from start to finish and included time for repeat sequences or patient adjustments.
(2) *Total sequence time* represented the sum of all the individual sequence times sent to the picture archiving and communication system (PACS) for the examina-

tion (this included all other sequences that were collected during the child's exam and included diffusion-weighted imaging and additional sequence planes that varied among the indication-based protocols). The total sequence time did not include time spent between sequences for technical setup, adjustment of patients/coils, sequences that were stopped before completion and not archived, and time for contrast or other medication administration between acquisitions (unlike total exam time).

(3) *Individual sequence times* were calculated for the axial T2-W and contrast-enhanced T1-W acquisitions and compared.

Statistical analysis

We used a Shapiro-Wilk test to test for normal distribution of the data. In cases with normal distributions, we summarized data by mean ± standard deviation; otherwise we summarized the data as median (interquartile range). For categorical variables, we used the Pearson chi-square test; for continuous variables, we used a Wilcoxon rank sum test to test the null hypothesis that there were no significant differences between the free-breathing and breath-held acquisitions. A *P*-value of less than 0.05 was considered statistically significant. We used the Cohen kappa coefficient to assess the interclass correlation coefficient (ICC) with the following scale of agreement: almost perfect (0.8–1.0), substantial (0.6–0.8), moderate (0.4–0.6), fair (0.2–0.4), slight (0.0–0.2) and poor (<0.0).

Results

Patient demographics are summarized in Table 2, with the most frequent clinical indications being mass (n=21), or vascular malformations (n=14) and button battery ingestion (n=7). In terms of body part, there were comparable numbers of chest and abdomen examinations across both groups (chest free-breathing 40.9% vs. chest breath-hold 47.8%). With regard to anesthesia and sedation techniques, the 22 breath-hold patients (including 4 neonates) all underwent MRI following general anesthesia with endotracheal intubation. Of the 23 children in the free-breathing radial group, 5 were neonates (<3 months of age) and were fed and swaddled for their MRI, 15 infants were sedated with intravenous propofol without endotracheal intubation and 3 infants underwent general anesthesia with endotracheal intubation for a combined MRI and surgical procedure.

There was a total of 535 anatomical landmark scores across both cohorts. The average score between the two readers is tabulated in Table 3 and summarized next.

Chest

Representative images for free-breathing and breath-held chest exams are shown in Fig. 1 along with their corresponding overall scores. Graphical and tabular summaries of the chest scores for T1-W and T2-W imaging are shown in Fig. 2 and Table 3. Both T2-W SSFSE and radial T2-W sequences performed well in their cohorts (overall mean imaging scores >3), with insignificant but higher overall imaging score observed with the radial T2-W sequence as compared with the T2-W SSFSE sequence (3.6 compared with 3.2, respectively, P=0.07). For the individual anatomical landmark scores, the trachea and lungs were significantly better visualized with the radial T2-W sequences (P=0.04 and P<0.01, respectively). For the contrast-enhanced T1-W sequences, there were also higher overall scores in the free-breathing cohort, but this did not reach statistical significance (4.0 compared with 3.0, P=0.06). The thymus, lungs and pulmonary arteries were all significantly better visualized on the 3-D radial sequence (P=0.02, P=0.03 and P=0.005, respectively). No thoracic structures were better visualized on either breath-held T1-W or T2-W sequences. There was also no significant difference in motion artifacts between sequences (P=0.39 for T1-W and P=0.73 for T2-W images).

Abdomen

Representative images for free-breathing and breath-held abdomen exams are shown in Fig. 3. Abdomen scores for T1-W and T2-W imaging are shown in Fig. 4. For the T2-W sequences, there was no significant difference in the overall imaging scores (T2-W SSFSE mean 3.7 compared with radial T2-W mean 3.9, P=0.66). For the individual landmarks, the adrenal gland was the only structure that was significantly better visualized on the radial T2-W sequences (P<0.01). For the contrast-enhanced T1-W sequences, although there was no significant difference in the overall imaging scores between the two cohorts, or among the individual anatomical landmarks, the pancreas was better visualized on the T1-W mDixon than the 3-D radial (P=0.03).

Artifacts encountered were low in incidence for both cohorts (mean motion artifact score was greater than 3.8 for both cohorts) with significantly increased motion artifacts encountered on the abdomen T2-W radial sequences (T2-W SSFSE mean of 4.7 compared with T2-W radial mean of 4.0, P<0.001).

Neonates

We performed a sub-analysis of the small number of neonatal exams, and representative images are shown in Fig. 5. The overall imaging score for the feed-and-swaddle

Table 3 Mean ± standard deviation of scores between readers as a function of exam sequence and anatomical landmark[a]

Sequences and anatomical landmarks	Abdomen			Chest		
	Breath-hold (*n*=13)	Free-breathing (*n*=12)	*P*-value[b]	Breath-hold (*n*=9)	Free-breathing (*n*=11)	*P*-value[b]
T2-W						
Motion artifact	4.7±0.7	4.0±0.6	**<0.001**	3.6±1.1	3.7±1.0	0.73
Main portal vein	4.0±0.9	4.5±0.4	0.18			
Diaphragmatic crura	4.0±0.6	3.9±0.4	0.49			
Pancreas	3.4±0.8	3.4±0.6	0.87			
Right/left adrenal	2.4±0.8	3.5±0.7	**<0.01**			
Spinal canal	3.8±0.9	4.0±0.5	0.45	3.5±0.9	3.5±1.0	0.90
Pulmonary arteries				3.0±0.8	3.5±0.9	0.23
Trachea				3.2±0.6	3.8±0.6	**0.04[c]**
Lungs				2.7±0.6	3.4±0.4	**<0.01**
Thymus				3.7±0.8	4.0±0.5	0.37
Overall	3.7±0.5	3.9±0.3	0.66	3.2±0.4	3.6±0.5	0.068
Contrast-enhanced T1-W						
Motion artifact	4.3±0.6	3.8±0.8	0.15	3.0±1.8	4.0±0.7	0.39
Main portal vein	4.7±0.6	4.2±0.8	0.06			
Diaphragmatic crura	4.5±0.5	4.3±0.7	0.46			
Pancreas	3.5±0.6	3.0±0.6	**0.03[c]**			
Right/left adrenal	3.6±0.6	3.9±0.9	0.23			
Spinal canal	3.5±0.7	3.4±0.6	0.56	3.2±1.1	3.4±0.4	0.74
Pulmonary arteries				2.7±1.3	4.5±0.7	**<0.01**
Trachea				3.6±0.7	4.1±0.2	0.10
Lungs				3.1±0.9	3.8±0.3	**0.03[c]**
Thymus				3.1±1.4	4.6±0.5	**0.02**
Overall	4.0±0.4	3.6±0.8	0.16	3.0±1.1	4.0±0.3	0.06

[a]Values shown are the average of the two readers

[b]$P<0.05$ is significant (bold)

[c]Indicates where statistical power is below a threshold of 80% as determined by cohort sample size

examinations using radial T2-W sequences was not statistically different from either the total breath-hold group (encompassing all ages) (T2-W SSFSE mean of 3.3 compared with radial T2-W mean of 3.8, P=0.06) or an age-matched group of breath-held neonates (P=0.15). Similarly, there was no difference in the overall imaging scores in the feed-and-swaddle contrast-enhanced T1-W sequences using 3-D radial imaging from the breath-held T1-W sequence (T1 mDixon mean of 3.5 compared with 3-D radial mean of 3.8, P=0.20) or the age-matched breath-held neonates (T1 mDixon mean of 2.9 compared with 3-D radial mean of 3.8, P=0.07). Motion artifact scores across the age-matched groups were also not significantly different for the T2-W sequences (T2-W SSFSE mean of 4.0 compared with radial T2-W mean of 3.6, P=0.30) or for the contrast-enhanced T1-W sequences (T1-W mDixon mean of 4.3 compared with 3-D radial mean of 4.2, P=0.70).

Interobserver variability

Cohen kappa for the intraclass correlation coefficient (ICC) between the two observers across the range of 535 anatomical landmark scores was 0.69 (95% confidence interval [CI] = 0.60, 0.77), indicating substantial agreement. Online Supplementary Material 1 shows the Cohen kappa as a function of anatomical landmark.

Exam time

As expected, the free-breathing T1-W and T2-W sequences took longer to acquire than their breath-hold comparisons; the median acquisition time of the T2-W radial sequences

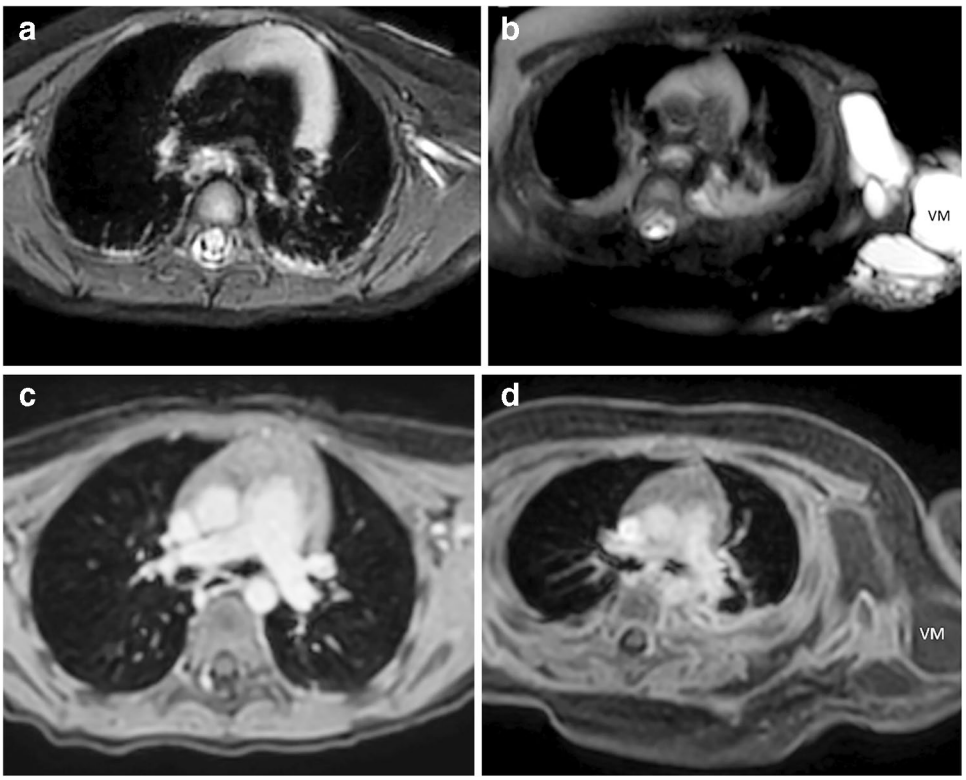

Fig. 1 Chest imaging examples and their scores. **a** Free-breathing axial radial T2-W fat-saturated MRI performed with intravenous sedation in a 7-month-old girl following button battery ingestion. The overall imaging score for the T2 sequence was 4.6. **b** Breath-held axial T2-W single-shot fast spin-echo (SSFSE) MRI performed with general anesthesia in a 6-month-old girl with vascular malformation (*VM*). The overall score for the T2 sequence was 3.8. **c** Axial contrast-enhanced T1-W 3-D radial MRI performed with intravenous sedation in same infant as (**a**), with an overall imaging score of 4.6. **d** Breath-held axial T1-W modified Dixon MRI performed with general anesthesia in same infant as (**b**). The overall imaging score was 4.2. *FS* fat saturated

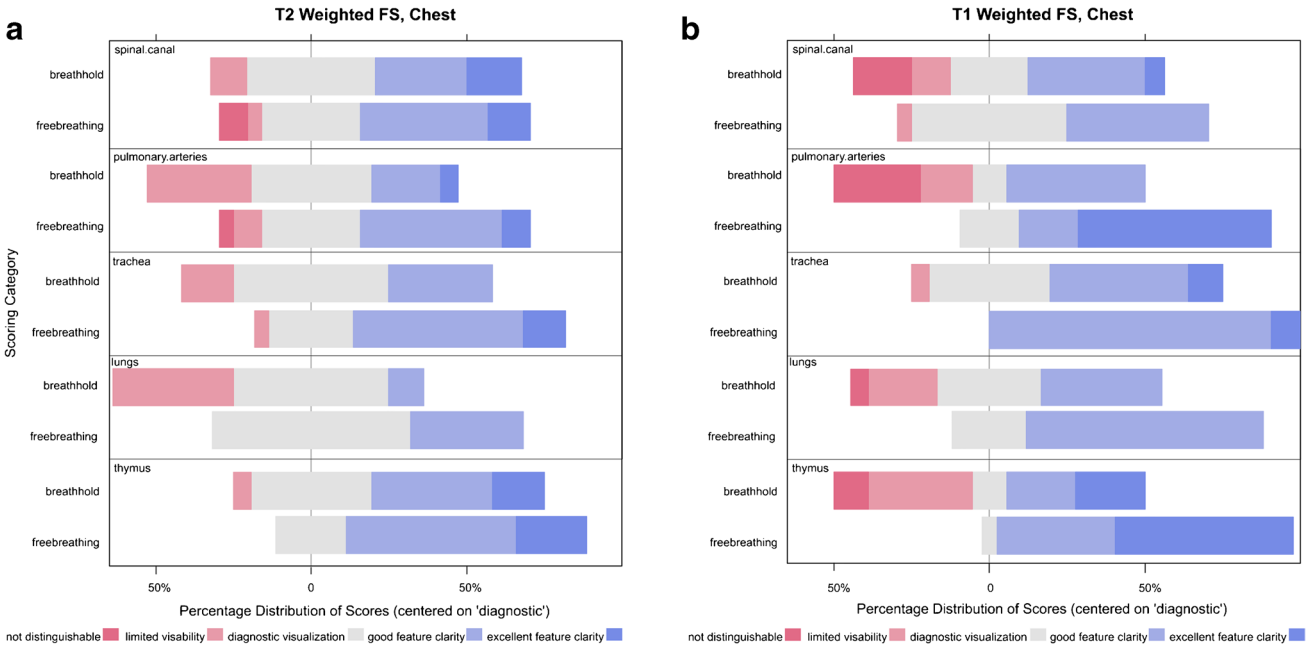

Fig. 2 Scoring distribution for chest imaging. **a, b** Graphs show scoring distribution of T2-weighted (**a**) and T1-weighted (**b**) MRI individual landmark scores as a function of the percentages of all scores

was 2.1 min longer than the median of the breath-hold T2-W sequences, and the median acquisition time of the 3-D radial sequences was 1.7 min longer than that of the breath-hold T1-W sequences (Table 1). The distribution of overall exam times for the free-breathing and breath-hold cases is shown in Table 4 and Fig. 6. In summary, the mean total exam time for free-breathing studies was not significantly different from the mean in breath-hold studies (P=0.94). Sub-analysis of the exam types found that the neonatal group with feed-and-swaddle (n=5) technique

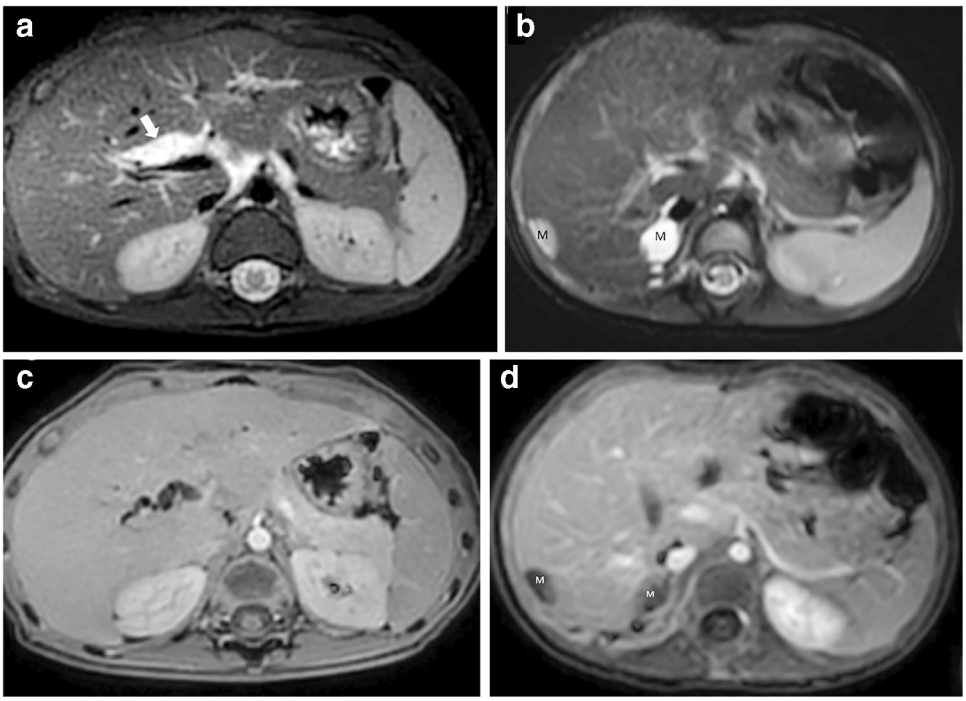

Fig. 3 Abdomen imaging examples and their scores. **a** Free-breathing axial radial T2-W MRI with fat saturation performed with intravenous sedation in a 24-month-old boy shows a dilated intrahepatic duct (*arrow*). The overall imaging score for the T2 sequence was 4.6. **b** Breath-held axial T2-W single-shot fast spin-echo (SSFSE) MRI performed with general anesthesia in a 29-month-old boy with lipoblastoma and retroperitoneal and subcapsular hepatic metastases (*M*). The imaging score for the T2 sequence was 3.8. **c** Axial contrast-enhanced T1-W 3-D radial MRI performed with intravenous sedation in same infant as (**a**), with an imaging score of 4.6. **d** Breath-hold axial T1-W modified Dixon performed with general anesthesia in same infant as (**b**), with an imaging score of 4.2

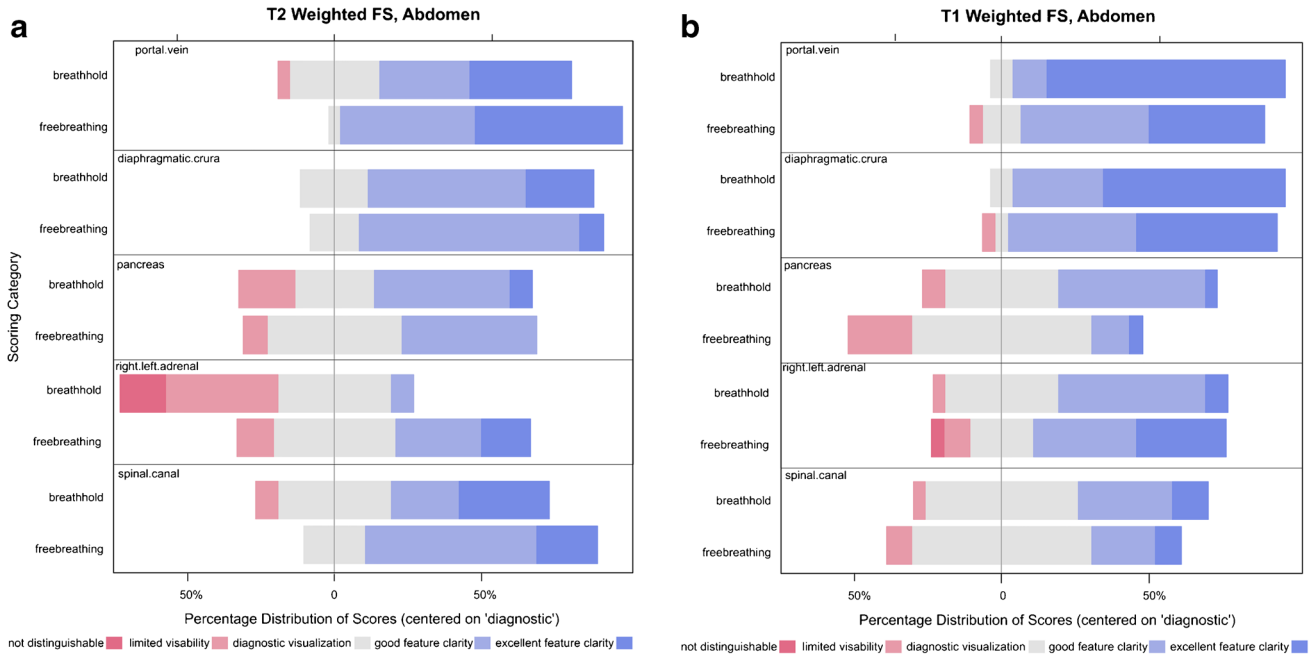

Fig. 4 Scoring distribution for abdomen imaging. **a, b** Graphs show score distribution for T2-weighted (**a**) and T1-weighted (**b**) MRI individual landmark scores as a function of the percentages of all scores

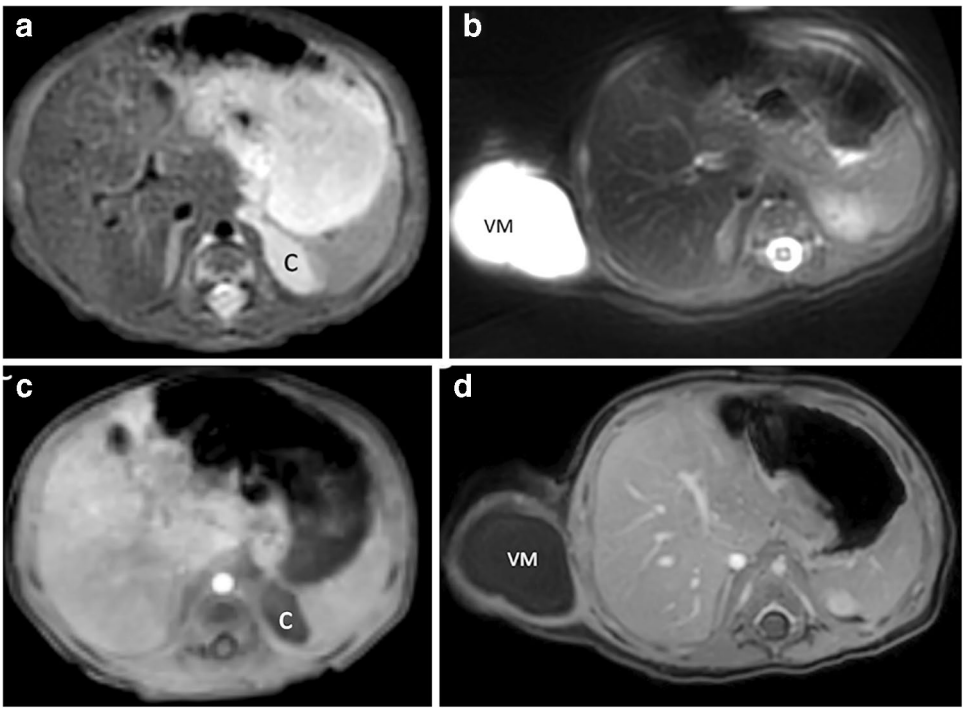

Fig. 5 Neonatal imaging examples and their scores. **a** Free-breathing axial radial T2-W fat-saturated MRI performed with swaddling in a 9-day-old boy with a right adrenal mass cyst (*C*). The overall imaging score for the T2-W sequence was 3.8. **b** Breath-hold axial T2-W single-shot fast spin-echo (SSFSE) MRI performed with general anesthesia in a 1-month-old boy with vascular malformation (*VM*), with an imaging score for the T2 sequence of 3.4. **c** Axial contrast-enhanced T1-W 3-D radial image obtained with intravenous sedation in same infant as (**a**), with an overall imaging score of 3.4. **d** Breath-held axial T1-W modified Dixon image obtained with general anesthesia in same infant as (**b**), with an overall imaging score of 4.0

Table 4 Exam time and sequence time comparison across both breath-holding and free-breathing cohorts

Studies	Breath-hold (n=22)[a]	Free-breathing (n=23)[a]	P-value[b]
Median total exam time, min			
All studies	48.5 (43.2, 54.9)	48.0 (42.2, 56.6)	P=0.94
Chest only	49.1 (44.2, 59.8)	49.0 (42.2, 56.6)	P=0.86
Abdomen only	48.3 (42.2, 53.3)	47.8 (43.8, 52.7)	P=0.80
Neonates only	47.8 (43.5, 52.2)	44.6 (37.5, 80.2)	P=1.00
Median total sequence time, min			
All studies	9.5 (6.3, 16.9)	18.2 (13.8, 21.0)	**P<0.01**
Chest only	12.8 (6.4, 28.7)	18.3 (13.8, 24.5)	P=0.46
Abdomen only	9.2 (6.8, 10.8)	17.6 (14.5, 20.4)	**P<0.001**
Neonates only	12.6 (8.1, 17.5)	14.7 (9.9, 15.1)	P=0.90
Median utilized sequence time, min			
All studies	1.3 (0.8, 2.8)	4.6 (3.8, 5.8)	**P<0.01**
Chest only	4.6 (1.0, 11.8)	4.6 (4.1, 5.4)	P=0.97
Abdomen only	1.1 (0.8, 1.7)	4.7 (3.6, 5.8)	**P<0.001**
Neonates only	1.7 (1.5, 2.0)	4.1 (3.9, 4.6)	**P=0.04**

[a]Median (interquartile range)

[b]P<0.05 is significant (bold)

had exam times lasting an average of 16.8 min longer than their breath-held general anesthesia counterparts. There was large variation in the total exam time for both cohorts, with the greatest variability found in the free-breathing cohort. The shortest breath-hold study lasted 27 min and the shortest free-breathing study took 29 min. The longest breath-hold study was 86 min and the longest free-breathing study (feed and swaddle) was 83 min. Both of these exams were outliers when compared to the other examinations (Fig. 6). There was also a notable difference between total exam times and the total sequence times for both the free-breathing and breath-hold techniques. This suggests that considerable time was spent during both cohorts adjusting sequence parameters and patient factors (including repositioning/airway management/reswaddling/contrast administration). The group with the largest difference between exam time and the summed sequence times was the neonatal feed-and-swaddle cohort, which had a mean difference of 41.8 min, likely because of repeat feeding and swaddling when the baby awoke.

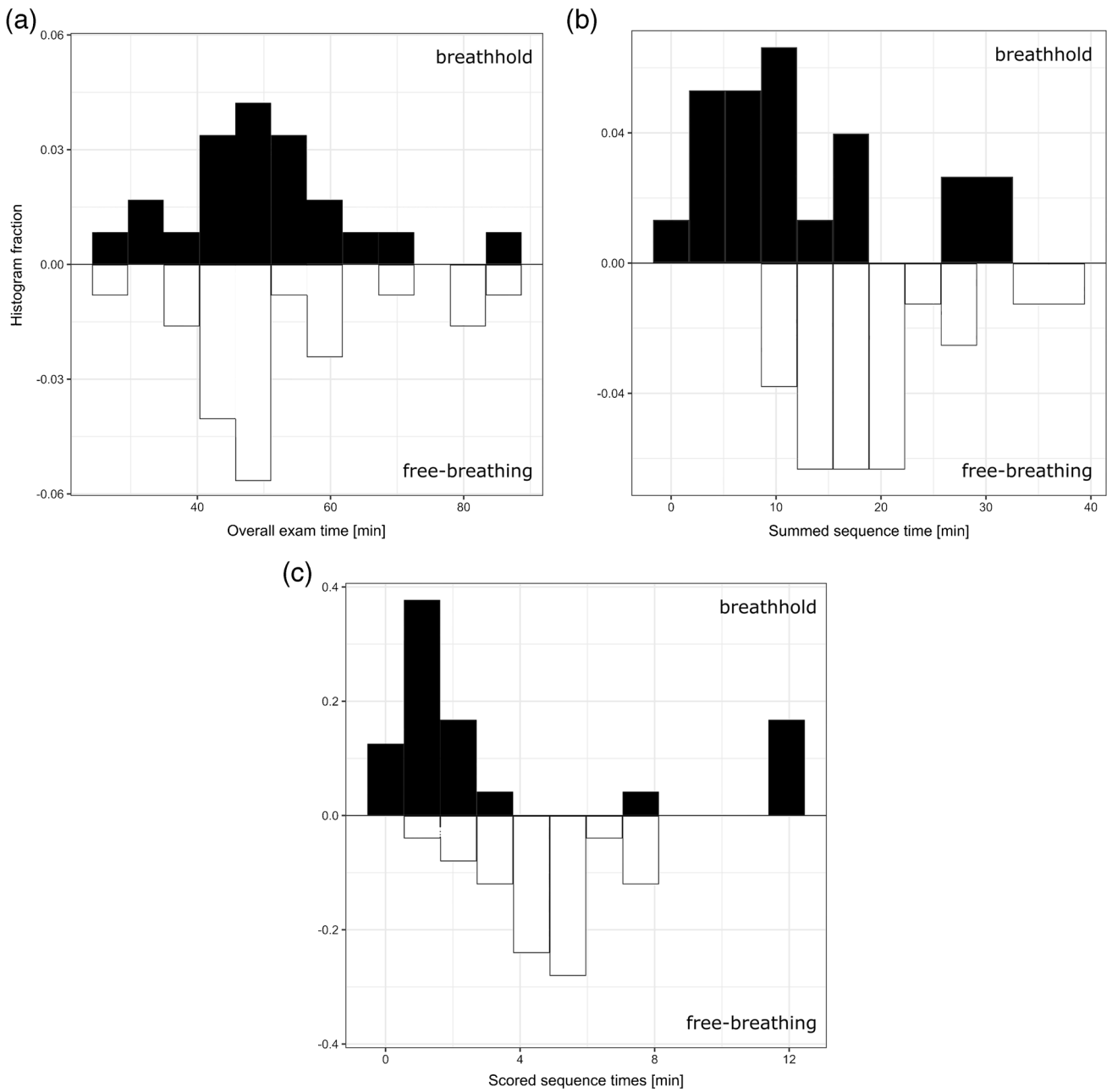

Fig. 6 Comparison of histograms representing exam and sequence duration times for the breath-hold and free-breathing approaches. **a–c** Histograms of the (**a**) exam, (**b**) sequence and (**c**) scored sequence times are shown for breath-hold studies on the positive y-axis and the freebreathing studies on the negative y-axis. The distribution of the overall exam times is similar and shows a few outliers with especially long scan times in both cohorts, but the free-breathing sequences trend longer, with the mean of the scored sequences being significantly different. Possible reasons for the comparable overall exam times could be related to the need for breath-hold instructions, required time between breath-holds for oxygen recovery, or need to repeat breath-hold sequences because of decreased sedation and respiratory paralysis level as medications are metabolized

Discussion

During the first 3 years after birth, 10% of children in developed countries undergo a general anesthetic for a medical, diagnostic or surgical procedure [2]. In December 2016, following results from animal studies, the U.S. Food and Drug Administration issued a warning that repeated or lengthy use of general anesthetic and sedation drugs during surgeries or procedures in children younger than 3 years might affect brain development, and subsequently issued labeling changes to these agents in April 2017 [2, 3]. Since that time, there have been conflicting results in human investigations

of a potential association between general anesthesia neurotoxicity in early life and longer-term neurodevelopmental outcomes [4–7]. While ongoing large-scale randomized controlled trials are being conducted, parental and provider concerns regarding the safety of these agents persist and necessary exams might be delayed in a misguided attempt to avoid general anesthesia. Irrespective of longer-term anesthesia neurocognitive effects, short-term adverse events from MRI-related anesthesia have been well described in the literature: infants younger than 1 year, infants who were born preterm, those with pulmonary or cardiac disease, and those with a higher American Society of Anesthesiology status (ASA>3) are at higher risk of hypoxemia and hemodynamic instability [9–12]. In addition, when an adverse event occurs, the unique challenges of the MRI environment can complicate resuscitation efforts [10, 11]. Despite the fact that most children who undergo MRI-related anesthesia do so without any short-term or lasting effects, any opportunity to reduce the degree and duration of sedation/anesthesia or eliminate it entirely is beneficial to the patient. For these reasons, applying motion-robust, accelerated imaging methods in pediatric patients has become a primary objective [13–18].

PROPELLER, or blade techniques with motion correction, have been shown to be robust to motion in adults across the body, including the most motion-challenging areas such as the heart and lungs [21–29]. In pediatrics, the approach first emerged as a technique to reduce motion in pediatric brain MRI [30], but relatively few articles have evaluated its use for pediatric body MRI [24, 31] and none has described its application in neonates and infants. Our study evaluated the performance of this approach in challenging scenarios, including awake neonates with large potential for motion degradation. The introduction of free-breathing radial sequences to our protocols had a dramatic effect on our pediatric imaging program, producing images that exceeded our previous experimentations with free-breathing Cartesian sequences [32]. This resulted in an immediate effect on reducing the need, duration and degree of sedation used in our patients, including non-sedated neonatal imaging and near-elimination of the need for invasive airway intubation in sedated infants. This study demonstrates that the decrease in sedation degree, time or need did not come at the expense of image quality, and in some cases the radial free-breathing exams exhibited improved diagnostic quality over the conventional breath-held T2-W and contrast-enhanced T1-W studies performed with the gold standard of general anesthesia. Interestingly, motion artifacts were minimal to none in the resulting images, despite the decreased sedation level, lack of paralytics and the neonatal feed-and-swaddle technique.

The reduction in general anesthesia and intubation were obtained at the expense of increased and widely variable imaging times; however, overall exam time was not prolonged by free-breathing radial approaches. Some sequences and exams in both cohorts were obvious outliers in terms of acquisition times. The reasons for these surprisingly long acquisition times were not recorded, but we can surmise based upon experience that they were caused by an intermittent technical/patient-related complication during acquisition. Patient-related complications such as desaturation and hypotension occur relatively frequently in this population and necessitate careful management because of the fragility of these children's physiology. Anesthesia and paralytic agents in the anesthesia group sometimes need to be readministered, and it is likely that unsedated neonates in this cohort might have awoken. A surprise result from this study was the considerable dead-time between sequences that was highlighted by the large differences between total exam time and total sequence time. There are likely many contributors to this dead-time in the scanner. In addition to physiological instability in sick neonates and infants necessitating evaluation, technical difficulties are very common in this age group and include problems with oxygen and blood pressure monitoring and intravenous access failure. These complications are rarely reported in the medical record because of their frequency of occurrence, but the high incidence highlights the importance of decreasing sedation. Now that we have demonstrated comparable imaging quality with robust motion-sensitive techniques, future efforts can work to speed up the free-breathing acquisitions.

Feed and swaddle

To attain sequence homogeneity in this study, we only included feed-and-swaddle exams that had contrast-enhanced T1-W imaging, limiting the overall volume of neonates in this study. In practice, our clinical protocol is to avoid intravenous contrast agent for our feed-and-swaddle MRI chest and abdomen cases where possible to limit interventions that might wake the sleeping neonate and to minimize exam time.

Limitations

Limitations of this study include its retrospective nature with different MRI sequences between the two patient groups. Modification of image acquisition parameters evolved as our experience with these novel sequences and feed-and-swaddle technique increased over the study period. However, the fundamental scan parameters across the two patient groups were similar and did not change across the study period (Table 1). There are slight differences in patient demographics between the two groups, with a slightly younger mean age in the free-breathing group, which was the result of increased referral of neonates to MRI following introduction of this free-breathing algorithm during our study period. Additional

confounders in this study include low patient number, MRI signal strength variations and the inevitable different physiological states between the two patient groups. These factors are impossible to completely untangle from changes in MRI sequences alone; however, this represents a real-life implementation of a technical advancement, which should translate well across pediatric radiology practices. Adverse incidents related to general anesthesia/sedation were not recorded in this study. Overall patient numbers were low and ultimately limit detailed statistical and power analysis where insignificant differences were seen. Statistical analysis was further limited by the inherently subjective nature of qualitative analysis between scorers, although ICC analysis was reassuring. Neonatal exams are underrepresented in this study because neonates who underwent feed-and-swaddle exams without contrast agent (most of our neonatal exams) were excluded to facilitate anatomical landmark evaluation on T1-W examinations, which was not reliable when using non-contrast-enhanced T1-W sequences. Also, neonates who underwent feed-and-swaddle exams and required more than one MRI appointment attempt were excluded, even if the second attempt was successful.

Conclusion

Free-breathing MRI chest and abdominal imaging using radial sequences can be performed successfully in infants and neonates. Free-breathing MRI exams provide comparable image quality to breath-holding examinations, facilitating unsedated neonatal imaging and reductions in the degree of sedation and airway intubation in infants. Our findings have allowed institutional implementation of free-breathing MRI techniques in young children undergoing chest and abdominal MR imaging, thereby reducing anesthesia, airway instrumentation, imaging cost and risk of anesthetic-related complications.

Supplementary Information The online version contains supplementary material available at https://doi.org/10.1007/s00247-022-05298-7.

Declarations

Conflicts of interest Quin Lu is an employee of Philips Healthcare. The remaining authors have no conflicts or competing interests relevant to this paper.

References

1. Huang YY, Ing C, Li G, Sun LS (2016) Analysis of MRI utilization in pediatric patients. J Neurosurg Anesthesiol 28:413–418
2. Shi Y, Hu D, Rodgers EL et al (2018) Epidemiology of general anesthesia prior to age 3 in a population-based birth cohort. Paediatr Anaesth 28:513–519
3. United States Food and Drug Administration (2016) FDA drug safety communication: FDA review results in new warnings about using general anesthetics and sedation drugs in young children and pregnant women. https://www.fda.gov/drugs/drug-safety-and-availability/fda-drug-safety-communication-fda-review-results-new-warnings-about-using-general-anesthetics-and. Accessed 3 Jan 2022
4. United States Food and Drug Administration (2017) FDA drug safety communication: FDA approves label changes for use of general anesthetic and sedation drugs in young children. https://www.fda.gov/drugs/drug-safety-and-availability/fda-drug-safety-communication-fda-approves-label-changes-use-general-anesthetic-and-sedation-drugs. Accessed 3 Jan 2022
5. Stratmann G, Sall JW, May LD et al (2010) Beyond anesthetic properties: the effects of isoflurane on brain cell death, neurogenesis, and long-term neurocognitive function. Anesth Analg 110:431–437
6. Davidson AJ, Sun LS (2018) Clinical evidence for any effect of anesthesia on the developing brain. Anesthesiology 128:840–853
7. Davidson AJ, Disma N, de Graaff JC et al (2016) Neurodevelopmental outcome at 2 years of age after general anaesthesia and awake-regional anaesthesia in infancy (GAS): an international multicentre, randomised controlled trial. Lancet 387:239–250
8. McCann ME, de Graaff JC, Dorris L et al (2019) Neurodevelopmental outcome at 5 years of age after general anaesthesia or awake-regional anaesthesia in infancy (GAS): an international, multicentre, randomised, controlled equivalence trial [published correction appears in Lancet 394:638]. Lancet 393:664–677
9. Malviya S, Voepel-Lewis T, Eldevik OP et al (2000) Sedation and general anaesthesia in children undergoing MRI and CT: adverse events and outcomes. Br J Anaesth 84:743–748
10. Cravero JP, Beach ML, Blike GT et al (2009) The incidence and nature of adverse events during pediatric sedation/anesthesia with propofol for procedures outside the operating room: a report from the pediatric sedation research consortium. Anesth Analg 108:795–804
11. Schulte-Uentrop L, Goepfert MS (2010) Anaesthesia or sedation for MRI in children. Curr Opin Anesthesiol 23:513–517
12. Dorfman AL, Odegard KC, Powell AJ et al (2007) Risk factors for adverse events during cardiovascular magnetic resonance in congenital heart disease. J Cardiovasc Magn Reson 9:793–798
13. Jaimes C, Gee MS (2016) Strategies to minimize sedation in pediatric body magnetic resonance imaging. Pediatr Radiol 46:916–927
14. Jaimes C, Kirsch JE, Gee MS (2018) Fast, free-breathing and motion-minimized techniques for pediatric body magnetic resonance imaging. Pediatr Radiol 48:1197–1208
15. Lee JH, Choi YH, Cheon JE et al (2015) Improved abdominal MRI in non-breath-holding children using a radial k-space sampling technique. Pediatr Radiol 45:840–846
16. Cheng JY, Zhang T, Ruangwattanapaisarn N et al (2015) Free-breathing pediatric MRI with nonrigid motion correction and acceleration. J Magn Reson Imaging 42:407–420
17. Ruangwattanapaisarn N, Loening AM, Saranathan M et al (2015) Faster pediatric 3-T abdominal magnetic resonance imaging: comparison between conventional and variable refocusing flip-angle single-shot fast spin-echo sequences. Pediatr Radiol 45:847–854
18. Zucker EJ, Cheng JY, Haldipur A et al (2018) Free-breathing pediatric chest MRI: performance of self-navigated golden-angle ordered conical ultrashort echo time acquisition. J Magn Reson Imaging 47:200–209
19. Hirokawa Y, Isoda H, Maetani YS et al (2008) Evaluation of motion correction effect and image quality with the periodically rotated overlapping parallel lines with enhanced reconstruction (PROPELLER) (BLADE) and parallel imaging acquisition technique in the upper abdomen. J Magn Reason Imaging 28:957–962

20. Chandarana H, Block TK, Rosenkrantz AB et al (2011) Free-breathing radial 3D fat-suppressed T1-weighted gradient echo sequence: a viable alternative for contrast-enhanced liver imaging in patients unable to suspend respiration. Investig Radiol 46:648–653
21. Pipe JG (1999) Motion correction with PROPELLER MRI: application to head motion and free-breathing cardiac imaging. Magn Reson Med 42:963
22. Hirokawa Y, Isoda H, Maetani YS et al (2008) MRI artifact reduction and quality improvement in the upper abdomen with PROPELLER and prospective acquisition correction (PACE) technique. AJR Am J Roentgenol 191:1154–1158
23. Liu J, Jin H, Chen Y et al (2021) Free-breathing BLADE acquisition method improves T2-weighted cardiac MR image quality compared with conventional breath-hold turbo spin-echo Cartesian acquisition. Acta Radiol 62:341–347
24. Choi KS, Choi YH, Cheon JE et al (2020) Application of T1-weighted BLADE sequence to abdominal magnetic resonance imaging of young children: a comparison with turbo spin echo sequence. Acta Radiol 61:1406–1413
25. Meier-Schroers M, Kukuk G, Homsi R et al (2016) MRI of the lung using the PROPELLER technique: artifact reduction, better image quality and improved nodule detection. Eur J Radiol 85:707–713
26. Zhang L, Tian C, Wang P et al (2015) Comparative study of image quality between axial T2-weighted BLADE and turbo spin-echo MRI of the upper abdomen on 3.0 T. Jpn J Radiol 33:585–590
27. Lane BF, Vandermeer FQ, Oz RC et al (2011) Comparison of sagittal T2-weighted BLADE and fast spin-echo MRI of the female pelvis for motion artifact and lesion detection. AJR Am J Roentgenol 197:W307–W313
28. Haneder S, Dinter D, Gutfleisch A et al (2011) Image quality of T2w-TSE of the abdomen and pelvis with Cartesian or BLADE-type k-space sampling: a retrospective interindividual comparison study. Eur J Radiol 79:177–182
29. Bayramoglu S, Kilickesmez O, Cimilli T et al (2010) T2-weighted MRI of the upper abdomen: comparison of four fat-suppressed T2-weighted sequences including PROPELLER (BLADE) technique. Acad Radiol 17:368–374
30. Vertinsky AT, Rubesova E, Krasnokutsky MV et al (2009) Performance of PROPELLER relative to standard FSE T2-weighted imaging in pediatric brain MRI. Pediatr Radiol 39:1038–1047
31. Zaccagnino E, Devincent C, Leelakanok N et al (2019) Assessment of quiet T2 weighted PROPELLER sequence in pediatric abdominal imaging. Clin Imaging 53:12–16
32. Balza R, Jaimes C, Risacher S et al (2019) Impact of a fast free-breathing 3-T abdominal MRI protocol on improving scan time and image quality for pediatric patients with tuberous sclerosis complex. Pediatr Radiol 49:1788–1797